Characterisation of the readout for the H.E.S.S.-I Upgrade

DESY Summer Student Program, 2014

Federica Bradascio

University of Pisa, Italy

Supervisors:

Stefan Klepser

Gianluca Giavitto

5^{th} of September 2014

Abstract

The High Energy Stereoscopic System (H.E.S.S.) - is an array of large atmospheric Cherenkov telescopes for very high energy (VHE, 100 GeV - 100 TeV) γ-ray astronomy. The H.E.S.S.-I camera upgrade project aims to increase the stability and performance of the camera operation by replacing the 10 years old electronics with modern-day technologies. This report focuses on the characterization of the new readout electronics and its integration with the existing photodetectors. C++ programs have been written for the acquisition and analysis of the data. The electronic noise of the readout was found to have two components. Measurements of single photoelectron spectra were used to determine the absolute gain of the photomultiplier tubes (PMT).

Contents

I Introduction **1**

II Theory and experimental method **2**
I The H.E.S.S. drawer 2
II The NECTAR chip 4
III Data structure 5
IV The Line DAC 6

III Measurements and Analysis **7**
I Pedestal measurement and noise identification 7
II Single Photoelectron (SPE) measurement 10
III Gain vs HV 11

IV Conclusions **13**

I. Introduction

The High Energy Stereoscopic System (H.E.S.S.) is an array of five imaging atmospheric Cherenkov telescopes located in Namibia, at 1800 meters altitude. It is dedicated to very high energy (VHE) γ-ray astronomy between 100 GeV and 100 TeV.

The initial four H.E.S.S. telescopes (Phase I) are arranged in the form of a square with 120 m side length, to provide multiple stereoscopic views of air showers. Each of these telescopes is composed of a 107m^2 mirror and a camera whose field of view is 5° in diameter. In Phase II of the project, a single huge dish with about 600m^2 mirror area was added at the center of the array, increasing the energy coverage, sensitivity and angular resolution of the instrument. [1]

In 2013 an upgrade project has begun for the cameras in the H.E.S.S.-I telescopes. The main goals of the upgrade are to increase the stability of the camera operation by replacing the 10-year old electronics with modern technologies (NECTAR chips, slimmer cabling, ethernet readout, filtered air circulation) and to reduce dead time in order to allow for higher readout rates.

All the components of the camera will be replaced after the upgrade, except for the photo-multiplier tubes and their bases. The main goal is to replace the readout electronics, upgrading the old analogue pipeline chip (ARS0) with the NECTAR chip, originally designed for the CTA project. The NECTAR chip features are:

- A longer analogue pipeline (1024 instead of 128 cells);
- A shorter readout time (5μs vs. 450μs);
- An integrated ADC.

The new electronics need to be tested before deployment: these tests are meant to probe functionality and ensure correct intercommunication of the hardware. Also, they are designed to check technical specifications (e.g. noise, linearity, gain, threshold)[2].

The aim of this project is to help characterize the readout of the H.E.S.S.-I upgrade, in order to verify the functionality of all the components. C++ programs have been written to acquire the data from experiments run during this project and to perform the data analysis, which has been done using ROOT framework.

II. Theory and experimental method

I. The H.E.S.S. drawer

The cameras of the H.E.S.S.-I telescopes combine a fine pixelization (for optimal imaging of the shower image) with fast electronics (for optimal background suppression). They comprise 960 photomultipliers tubes (PMT) arranged in drawers of 16 each, power supplies and the full trigger, readout and slow control electronics.

Figure 1: *The* H.E.S.S. *drawer.*

The electronics of the camera of the H.E.S.S. system are divided into two parts: the front-end electronics arranged in 60 *drawers* (see Figure 1) and the back-end electronics in a crate at the rear of the camera. Each of the 60 drawers contains 16 PMTs and associated acquisition and local trigger electronic cards. The analogue signals are digitized in the drawers and then the digital signals are sent to the acquisition crate. Figure 3 shows the new structure of a drawer, after the H.E.S.S.-I camera upgrade. Each drawer is composed of one *slow control board* and two *analogue boards*, each reading the data from 8 PMTs. Each analogue board has 8 NECTAR chips, each one connected to one PMT.

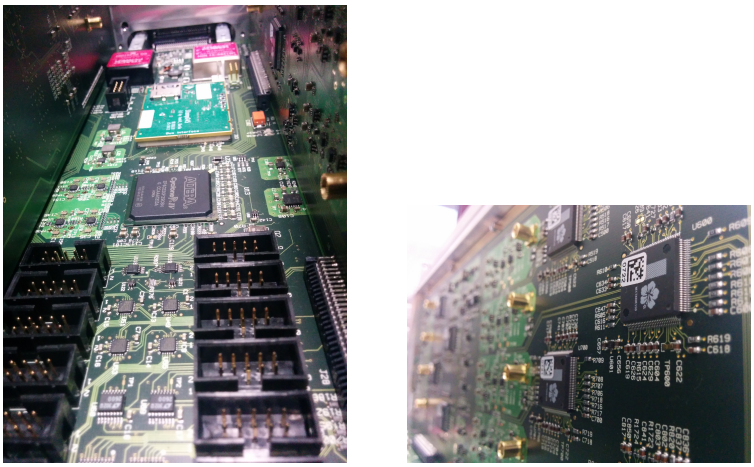

(a) (b)

Figure 2: *The slowboard (a) and the analogboard (b).*

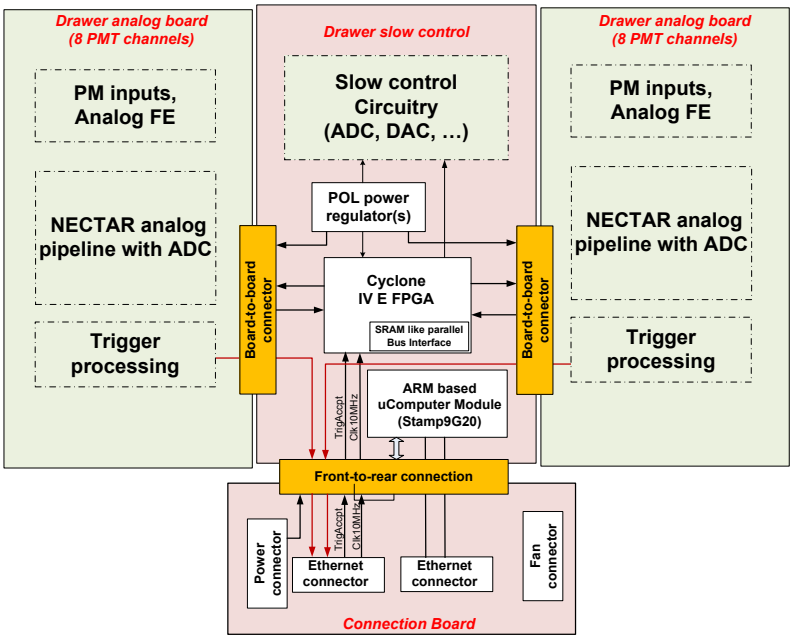

Figure 3: *The structure of the new drawers. The incoming data is digitized by the NECTAR chips, then goes to the FPGA, where a serialization is done. The ARM processor provides the Ethernet interface and the software interface to the higher level software.*

II. The NECTAR chip

The NECTAR chip (Figure 4) is a fast memory and digitizer chip: it contains a ring analogue memory, an analogue-to-digital-converter (ADC) and two amplifiers. Each chip has two channels, which in the H.E.S.S. upgrade electronics are fed by a single PMT signal with two different gains, a high gain (HG) and a low gain (LG). The sampling is performed at a rate of 2 GHz.

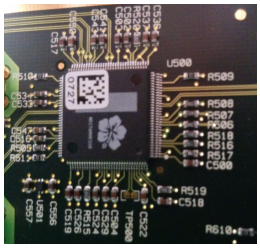

Figure 4: *The NECTAR chip.*

The analogue voltage levels are continouosly stored in a ring buffer consisting of 1024 capacitor cells (see Figure 5). On the occurrence of a trigger signal, this writing process is stopped and N_f samples of the ring buffer are digitized by a 20 MHz ADC, starting at a programmable readout offset N_d. The readout samples start from the cell with index FCR (First Cell to Read). This operation takes between $2 \div 3.2\mu$s (for $N_f = 16$ and 32, respectively). The digitized signals are then stored and processed in a field-programmable gate array (FPGA). An ARM-based embedded linux computer reads out the FPGA and forms the events that are then sent to a central computer for further processing.

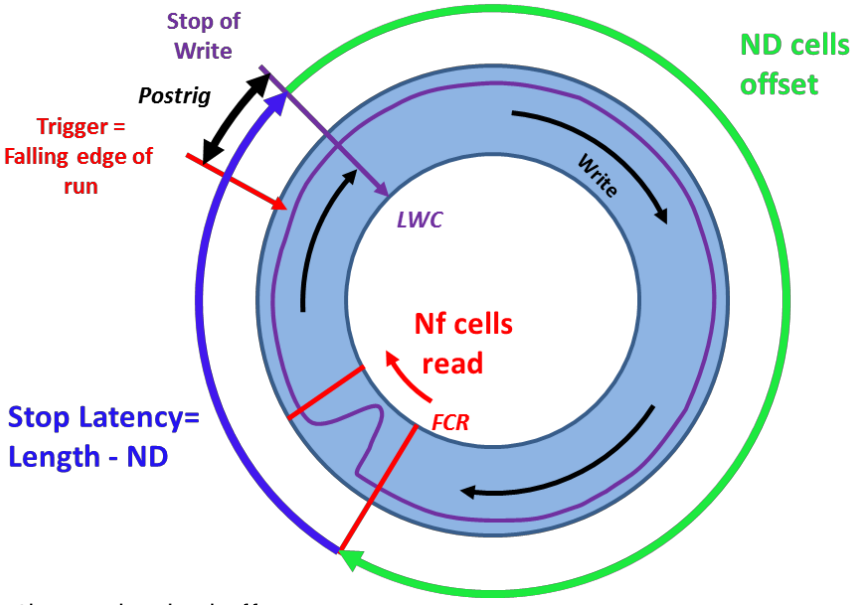

Figure 5: *Working principle of the analogue memory as circular buffer with flexible readout window.*

III. Data structure

Each event is structured in two parts: the control header and the 32 data samples. The header contains informations about the number of the event and the FCR. Each of the 32 samples consists of a short type identifier (ID) of 6 bits length, the sample number of 10 bit length, and 32 16-bit integers containing the ADC values of the NECTAR chips for that sample (16 HG and 16 LG). Here you can see the members of the *Event* class:

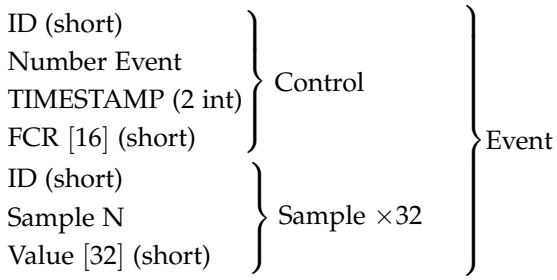

Because of this structure, a drawer event can be simply described using a C++ class. As you can see in Listing 1, the class *Event* has 6 public members and 3 methods.

Listing 1: *Drawer Event Class (C++)*

```
#define N_CH 32                                  //numbers of channels
#define N_SPL 32                                 //numbers of samples
#define LEN_FCR 16                               //FCR length
#define LEN_TSTAMP 2                             //TIMESTAMP lenght

class Event
{
    public:
    short ID_control;
    int Number_Event;
    int TIMESTAMP[LEN_TSTAMP];
    short FCR[LEN_FCR];
    short ID_sample,
    int Value[N_CH*N_SPL];
    void FillControl(short, int, int*);          /*method to fill the ID_control
                                                 Number_Event and TIMESTAMP*/
    void FillFCR(short*, int);                   // method to fill the FCR vector
    void FillSample(short, short*);              // method to fill the Value array
};
```

IV. The Line DAC

The structure of a NECTAR chip for each channel is a L×C matrix (L lines=16, C columns=64) of analogue storage cells. The analogue input is buffered by amplifiers providing the signal for each line. The sampling signal starts from the first cell of the first column and propagates along the column through a delay line loop. At the end of the column, it jumps to the beginning of the next one and so on. At the end of the matrix, it restarts from the first cell (circular buffer operation)[4].

As each line has its own input buffer, but also its readout amplifier, a spread of DC levels between lines is expected. This DC dispersion, which is stable in time, can be corrected offline or compensated using digital-to-analogue converters (DAC) associated to each line. The DACs are permitting to compensate for the dispersion of DC levels between lines.

The offline correction of the lines is provided by a C++ code. The following steps are executed:

1. A 3-D histogram is created: on the x axis there are the 16 channels (HG), on the y axis there are the 16 lines and on the z axis there are the sample values. The number of the line is given by its absolute sample number modulo 16.
2. 3 loops are done to fill the 3-D histogram: the first one is on the entries, the second one is on the channels and the last one is on the samples.
3. For each channel and each line, the 3-D histogram is projected on the z axis. In this way a 1-D histogram is created, which represents the section of the 3-D histogram.
4. The correction is given by the mean value of the 1-D histogram.
5. The corrected value (waveform histogram) is the sample value minus the correction.

In Figure 6 the 3-D histogram is shown, with the projection on the x and y axis: the line DAC provides a flat distribution of the samples around the value of 400 ADC counts.

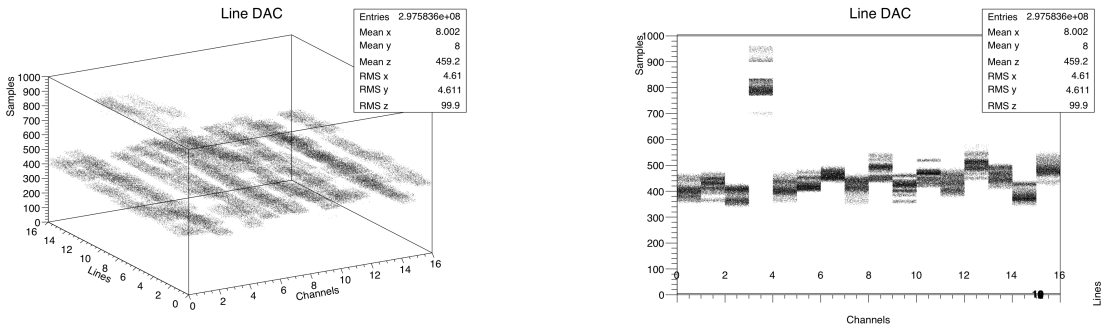

Figure 6: *Line DAC correction for the pedestal.*

III. Measurements and Analysis

I. Pedestal measurement and noise identification

The first step in the characterization of a complex and sensitive electronic apparatus such as the drawer, is the determination of its background electronic noise. To do this, it is important to perform a measurement of the distribution of the ADC charge recorded in the absence of any input signal, often called *pedestal*. The pedestal has non-zero width due to:

- PMT (e.g. the leakage current);
- electronic noise (e.g. shot noise);
- instrumental effects (e.g. periodic ripples from digital logic).

The first two processes can be described by a Gaussian [6].

The procedure to measure the pedestal is as follows: no light pulses is sent to the PMTs, the PMT high voltage (HV) is set to 1200 V and the trigger is sent to one channel via a signal generator (`81160A Pulse Function Arbitrary Generator, Agilent Technologies`). Then a C++ program is used to retrieve the charge and RMS distributions and the waveform.

The charge is obtained by summation of the 16 samples; Figure 7 shows its distribution for a pedestal run for channel 1. The charge distribution of the pedestal is too wide: the σ value is 34 ADC counts, while the nominal value is 16 ADC counts. Furthermore in logarithmic scale, the presence of outliers is evident.

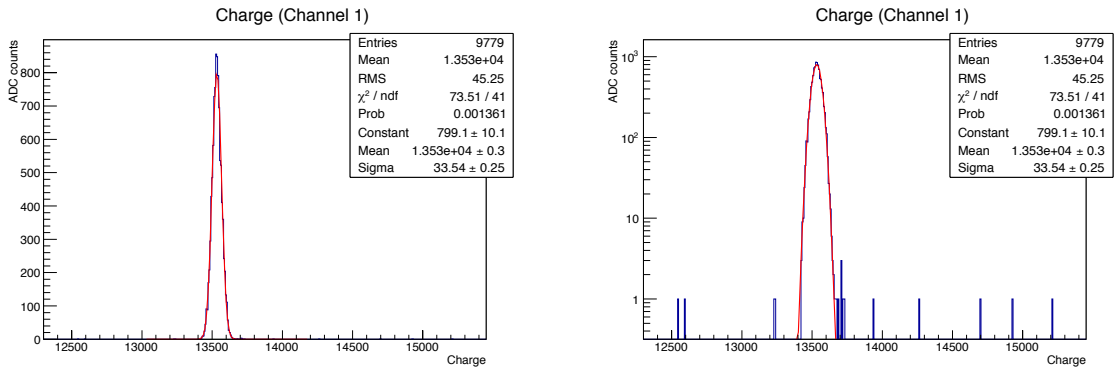

Figure 7: *Pedestal charge distribution of channels 1, fitted by a Gaussian. The graph on the left is in linear scale, that on the right is in logarithmic scale.*

The RMS distribution of the pedestal of channel 1 (Figure 8), is not a Gaussian, as it should be, but a bimodal distribution. The majority of events has an RMS of $\simeq$ 25 ADC counts, while $\sim$ 9%

has an RMS distributed around $\sim$ 35 ADC counts.

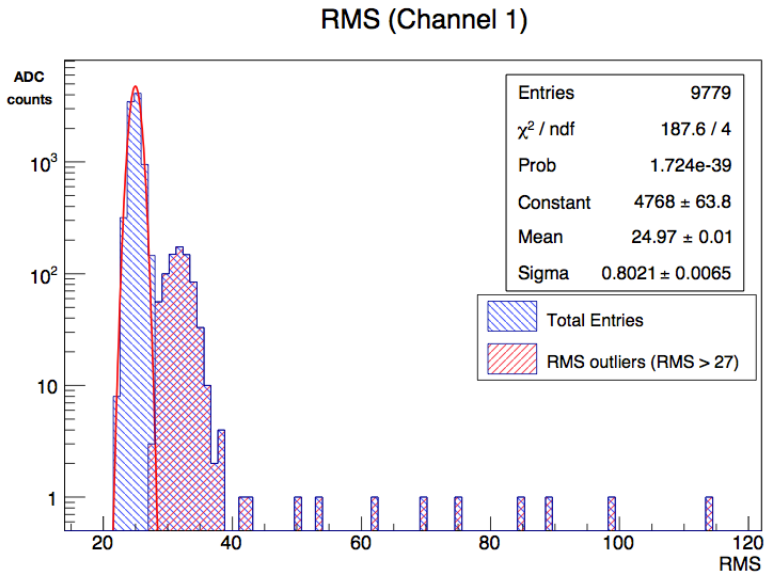

Figure 8: *Pedestal RMS distribution of channel 1. The Gaussian fit is done on the first peak. The blue area represents the total signal, the red area is the component with the increased noise.*

The waveform plot (time distribution of the events as function of the samples) of events with high RMS shows oscillations around the mean value (Figure 9).

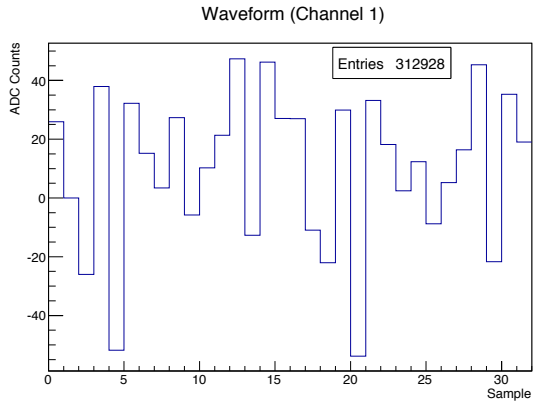

Figure 9: *The waveform for the channel 1.*

In order to have further informations about this noise, the charge distributions has been plotted as function of the RMS values: as shown in Figure 11, the charge is independent from the RMS. Therefore the noise is not correlated with the pedestal charge. From this measurements it turns out that the drawer is in general twice as noisy as nominal. There is a secondary component in the noise with higher RMS, which shows bunches of oscillations. Later these oscillations have been detected on the oscilloscope (see Figure 10). This secondary electrical noise component was found out to be caused by the electromagnetic interferences of the DC/DC converter. It was later corrected by substituting the DC/DC converter and the present pedestal distribution has a nominal width matching the specifications (Figure 12).

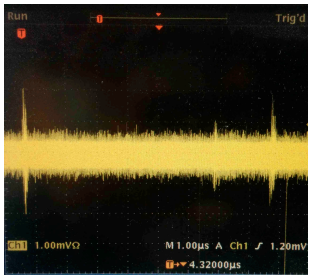

Figure 10: *Periodic noise seen at the oscilloscope.*

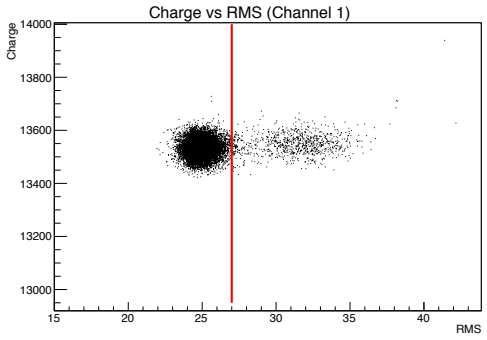

Figure 11: *Charge distribution as function of the RMS values. The denser zone on the left represents the first component, fitted by the Gaussian on Figure 8; the events with RMS > 27 are from the second component.*

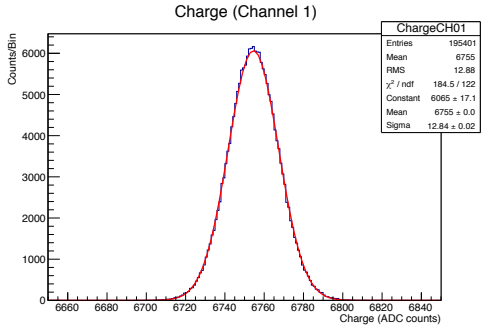

Figure 12: *Charge distribution of channel 1, after substituting the DC/DC converter. No more outliers are present and the width is within specifications.*

II. Single Photoelectron (SPE) measurement

In order to determine the mean number of detected photoelectrons by the PMTs, it is required a precise determination of the single-photoelectron response of the phototube. The single photoelectron (SPE) spectrum shows the response of the photomultiplier tube to a single photon source and is used for the absolute calibration of the camera, since if the response to a single photon is known it is possible to predict the response to higher intensity sources, because PMTs are linear devices. From the SPE spectrum the PMT gain can be extracted.

Without background noise the PMT response can be approximated as a convolution of a Poisson distribution and a Gaussian distribution, representing the number of photons hitting the photocatode and the response of the multiplicative dynode system respectively. In a real PMT , in addition to the process of conversion of light and subsequent amplification of charge, various background processes must also be taken into account. They generate additional charge (noise) and modify the output charge spectrum. Such noise signals in the anode circuit could be generated even in the absence of a light signal (pedestal) [6]. Therefore the real PMT spectrum is given by the convolution of the ideal spectrum and of the real one. The function obtained in this way by Bellamy *et al.* [6], can be approximated, if thermo-emission is negligible, to the following expression:

$$\begin{aligned}\mathcal{F}(x) =& N \times \left(\frac{e^{-\mu}}{\sqrt{2\pi}\sigma_P} \exp\left[-\frac{1}{2}\left(\frac{x-P}{\sigma_P} \right)^2 \right] + \right. \\ & \left. + k \sum_{n=1}^{m \gg 1} \frac{e^{-\mu}}{\sqrt{2\pi}\sigma_{\gamma_e}} \frac{\mu^n}{n!} \exp\left[-\frac{1}{2}\left(\frac{x-(P+n\gamma_e^{ADC})}{\sqrt{n}\sigma_{\gamma_e}} \right)^2 \right] \right)\end{aligned} \tag{1}$$

where the first term represents the pedestal distribution and the second one a Poisson distribution for the number of photo-electrons convoluted with Gaussian of increasing width, representing the resolution of the PMT for a signal of n photo-electrons. The electronic pedestal (first term) is approximated by a Gaussian with a standard deviation σ_P and with a mean position in ADC counts P. The light distribution for a given signal of n photoelectron is approximated also by a Gaussian with a standard deviation $\sqrt{n}\sigma_{\gamma_e}$ and with a mean position in ADC counts $P + n\gamma_e^{ADC}$, γ_e^{ADC} being the conversion factor between ADC counts and photoelectrons and σ_{γ_e} is the RMS of the charge induced by a single photoelectron. k is a normalization constant that characterize the compliance of the full distribution with a Poisson distribution. In the case of a true Poisson distribution, it should be equal to 1 [3].

In order to measure SPE distribution, light was sent on the PMTs using a dedicated SPE unit from the H.E.S.S. experiment. The drawer was placed in a light-tight dark box, to protect the PMTs from stray background light. The light is generated by the signal generator (`81160A Pulse Function Arbitrary Generator, Agilent Technologies`) at a fixed frequency of 400 Hz and sent to the channel 12. The pulse height is of 65 mV. The drawer is triggered in coincidence with the light pulse, via the signal generator, and attenuated by 16 dB (`H1/Langer TRILITHIC`,

BMA-581). A delay of 400 ns between the light signal and the trigger signal is set to match the arrival of the pulse to the readout window. 15 measurements have been done of 350 s each, changing the PMT HV from 850V until 1150V.

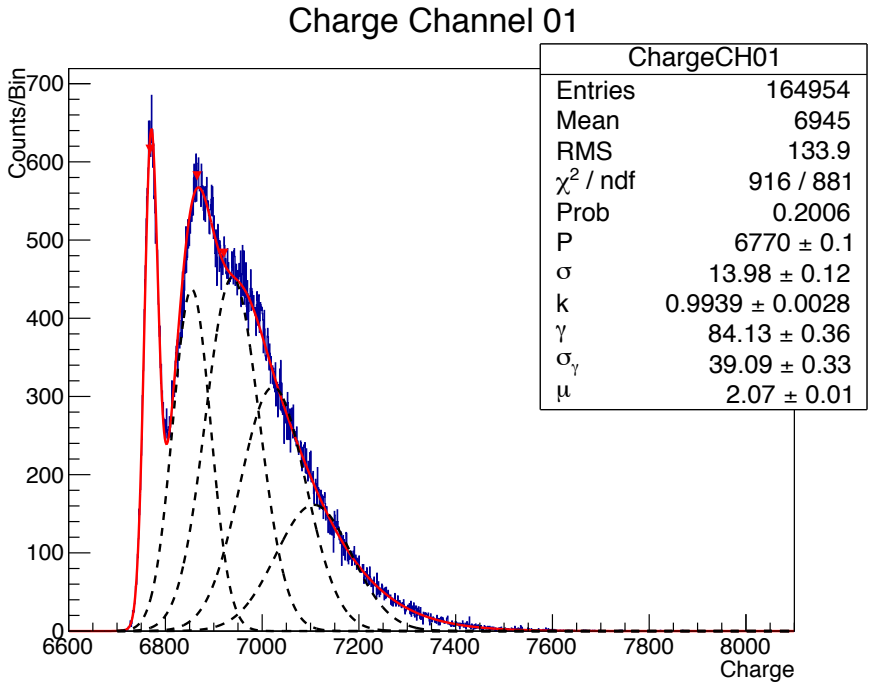

Figure 13: *ADC count distribution for a single-photoelectron run of the channel 1, at* 1150 *V. The dashed curves represent the partial charge distributions corresponding to n=1,2,3,4 photoelectrons emitted by the photocathode.*

For each HV and each channel, the SPE charge distribution is obtained and analyzed by means of a ROOT program based on the MINUIT numerical minimization program. The PMT response function (1) is used as the fitting function: all parameters are free except the overall normalization N which is fixed according to the number of events in the run. The gain γ_e^{ADC} is evaluated as the difference between the pedestal peak and the first photoelectron peak. In Figure 13 the SPE response of the PMT at 1150V is shown. The gain $\gamma = 84.1 \pm 0.4$ADC counts per photoelectron is close to the nominal value of 80 ADC counts per photoelectron.

III. Gain vs HV

The SPE fit has been performed for each channel and each PMT as described above. From the SPE fit, the gain value has been extracted and plotted as function of the HV , for each channel.

The Figure 14 shows it for channel 1. The gain grows linearily as function of the HV; for HV bigger than 1400V, the HG saturates. At HV lower than 1000V the fit fails. The errors appear to be underestimated.

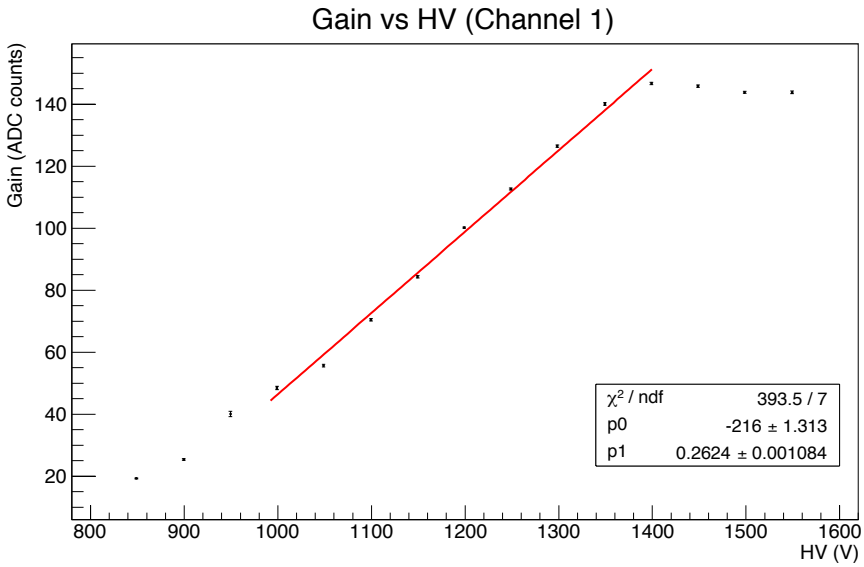

Figure 14: *ADC count distribution for a single-photoelectron run of the channel 1, at* 1150 *V.*

For each PMT the HV values at which the gain is $\sim$ 80ADC counts has been found, through linear interpolation. The values obtained are reported into Table 1.

Table 1: *Voltage for* $\gamma \sim 80$ *ADC counts per photoelectron.*

Channel	HV (V)	Channel	HV (V)
1	1135	8	1442
2	1268	9	890
4	942	11	1046
5	1404	12	1343
6	1036	13	1051
7	962	14	1098
		15	1223

IV. Conclusions

Early tests of pedestal noise showed presence of additional component and in general a bad performance of the readout. The problems were fixed during the course of the summer and now the performance is nominal.

For the first time the SPE spectrum was measured using a NECTAR -based readout. An HV scan was performed, finding the HV value at which $\gamma = 80$ADC countsfor 13 PMTs out of 16.

Acknowledgments

Foremost, I would like to express my sincere gratitude to my supervisor Gianluca Giavitto for the continuous support of my project at DESY, for his patience, motivation, enthusiasm, and immense knowledge. His guidance helped me to learn new things and to understand what a research does, but above all he made me fall in love with astroparticle physics. I could not have imagined having a better supervisor for my Summer Student. I would like to thank Stefan Klepser for inviting me to work with the HESS group at DESY, Valentine Lefranc and all the H.E.S.S. group for making me feel one of them.

References

[1] https://www.mpi-hd.mpg.de/hfm/HESS/

[2] Bolmont J. et al. *H.E.S.S. I Camera Upgrade Project*

[3] Aharonian, F. et al. *Calibration of cameras of the H.E.S.S. detector*, Astroparticle Physics 22, 109–125 (2004).

[4] E. Delagnes, *Specifications of the Nectar0 and NECTARHESS Chips*, private communication.

[5] Hyman, L. G., Schwarcz, R. M. & Schluter, R. A. *Study of High Speed Photomultiplier Systems*, Review of Scientific Instruments 35, 393–406 (1964).

[6] Bellamy, E. H. et al. *Absolute calibration and monitoring of a spectrometric channel using a photomultiplier*, Nuclear Instruments and Methods in Physics Research Section A: Accelerators, Spectrometers, Detectors and Associated Equipment 339, 468–476 (1994).